

Chlorophyll *b* to Chlorophyll *a* Energy Transfer Kinetics in the CP29 Antenna Complex: A Comparative Femtosecond Absorption Study between Native and Reconstituted Proteins

Roberta Croce,* Marc G. Müller,* Roberto Bassi,[†] and Alfred R. Holzwarth*

*Max-Planck-Institut für Strahlenchemie, Mülheim ad Ruhr, D-45470, Germany; and

[†]Dipartimento Scientifico e Tecnologico, Facoltà di Scienze, Strada le Grazie, I-37134 Verona, Italy

ABSTRACT The energy transfer processes between Chls *b* and Chls *a* have been studied in the minor antenna complex CP29 by femtosecond transient absorption spectroscopy. Two samples were analyzed: the native CP29, purified from higher plants, and the recombinant one, reconstituted *in vitro* with the full pigment complement. The measurements indicate that the transfer kinetics in the two samples are virtually identical, confirming that the reconstituted CP29 has the same spectroscopic properties as the native one. In particular, three lifetimes (150 fs, 1.2 ps, and 5–6 ps) were identified for Chl *b*-652 nm to Chl *a* energy transfer and at least one for Chl *b*-640 nm (600–800 fs). Considering that the complexes bind two Chls *b* per polypeptide, the observation of more than two lifetimes for the Chl *b* to Chl *a* energy transfer, in both samples, clearly indicates the presence of the so-called mixed Chl binding sites—sites which are not selective for Chl *a* or Chl *b*, but can accommodate either species. The kinetic components and spectra are assigned to specific Chl binding sites in the complex, which provides further information on the structural organization.

INTRODUCTION

The main functions of antenna complexes in higher plants are to absorb light and transfer excitation energy to the reaction centers for use in photosynthetic charge separation and also to control this energy flow to avoid possible photodamage (Van Amerongen and van Grondelle, 2001; Bassi and Caffarri, 2000). These proteins belong to the Lhc multigenic family (Jansson, 1999). Although all members share common features, each complex has specific biochemical, spectroscopic, and functional properties.

CP29 is one of the minor antenna complexes of Photosystem II (PS II). It is present in the supramolecular antenna of PS II in monomeric form and it is located between the reaction center and the major light-harvesting complex (Hankamer et al., 1997; Boekema et al., 1999). CP29 is the product of the nuclear gene *Lhcb4*. Its primary sequence is highly homologous to the other Lhc proteins, but shows an insertion of 42 amino acids at the N-terminal domain, where a phosphorylation site has been detected (Testi et al., 1996). Native CP29 binds eight chlorophylls (Chls): six Chls *a*, two Chls *b*, and two carotenoid molecules (Sandona et al., 1998). Reconstitution *in vitro* of the recombinant apoprotein with pigments allowed obtaining a complex with the same biochemical and spectroscopic properties of the protein as

purified from plants (Giuffra et al., 1996). Moreover, spectroscopic analysis of CP29 complexes reconstituted with different Chl *a/b* ratios suggested that some of the Chl binding sites are not selective and they can be occupied by either of the two Chl species (Giuffra et al., 1997). These results were confirmed by mutation analysis at the Chl-binding residues: for some of the mutants, although only one Chl per polypeptide was lost, the biochemical and spectroscopic data indicate that contributions of both Chl *a* and Chl *b* were involved (Bassi et al., 1999; Simonetto et al., 1999). In particular, four sites have been found to have mixed occupancy (A3/B3 and B5/B6 in the corresponding Kühlbrandt notation introduced for LHCII; Kühlbrandt et al., 1994). Some doubt still remains whether this effect is present also in the native complex, or if it is, in fact, the result of *in vitro* reconstitution where the folding process is probably different than *in vivo*.

The study of the energy transfer kinetics in CP29 can give an answer to this question: if the two Chls *b* of CP29 are accommodated in two sites, two lifetimes for the Chl *b* to Chl *a* energy transfer are expected. In contrast, if the two Chls *b* are coordinated to four binding sites, as the mutation analysis suggests, a higher number of components should be observed in the Chl *b* to Chl *a* energy transfer kinetics. It has also been possible to calculate the energy transfer processes in CP29 within a Förster model, since all the parameters involved in the Förster equation have been determined using various methods: the distance between the chromophores has been taken from the structure of the homologous protein LHCII (Kühlbrandt et al., 1994), the energy levels of the Chls have been determined from mutation analysis (Bassi et al. 1999) and the transition dipole moment orientations were determined from linear dichroism (LD) measurements on mutants lacking specific Chls (Simonetto et al., 1999). Although the Förster model can clearly

Submitted August 5, 2002, and accepted for publication December 6, 2002.

Address reprint requests to Dr. Roberta Croce, E-mail: roberta.croce@unimi.it; or to Prof. Alfred Holzwarth, E-mail: holzwarth@mpi-muelheim.mpg.de.

Roberta Croce's present address is Istituto di Biofisica, CNR sezione di Milano, Via Celoria 26, I-20133 Milano, Italy.

Abbreviations used: Chl, chlorophyll; DM, *n*-docecyl- β -D-maltoside; FWHM, full width half-maximum; LD, linear dichroism; nCP29, native CP29; rCP29, recombinant CP29.

© 2003 by the Biophysical Society

0006-3495/03/04/2508/09 \$2.00

only be a first order approximation to the kinetics, the spectra and transient absorption kinetics could be simulated reasonably well only when assuming a mixed site occupation (Cinque et al., 2000b).

Two other experimental studies on the energy transfer kinetics in CP29 have been published so far. The first femtosecond study (Gradinaru et al., 1998) showed that there are two main pathways for Chl b to Chl a energy transfer, with lifetimes of 350 fs and 2.2 ps. In a very simple model the first lifetime was assigned to the transfer from the “blue” Chl b (640 nm) to the “red” Chl a (680 nm), whereas the 2.2 ps signal was assigned to the transfer from the “red” Chl b (650 nm) to the blue Chl a (675 nm). Equilibration among Chls a was detected in 280 fs and 10–13 ps (Gradinaru et al., 1998). More recently the same group performed a new femtosecond study on CP29 focused mainly on Car to Chl energy transfer (Gradinaru et al., 2000) with an improved time resolution (<100 fs versus 200 fs) although some new information was also obtained on Chl-Chl transfer. The authors observed a faster transfer step from Chl b-640 nm with 220-fs lifetime, which account for 60% of the energy in the 640-nm form, whereas the main transfer from 652 nm Chl b was detected at 2.2-ps lifetime, and a second decay for the 640-nm Chl b was observed with a similar lifetime. Furthermore, a slow transfer from both Chl b spectral forms was observed with a \approx 10-ps lifetime. Additional information about Chl energy transfer in CP29 was obtained by hole burning: the energy transfer times, calculated from the zero-phonon hole widths at 4.2 K for Chl b 638.5 nm and Chl b 650 nm were 900 fs and 4.2 ps respectively, and the transfer from Chl a 665, 5.2 ps (Pieper et al., 2000).

In this work we present a femtosecond absorption study on the energy transfer processes at RT in both native and reconstituted CP29 complexes after preferential Chl b excitation. Besides further detailed analysis of the transfer paths, the aim of this article is also to compare the results in the two complexes to check if the kinetic parameters are conserved. In this way it will be possible to determine if the mixed sites also exist *in vivo*. If the same lifetimes for energy transfer can be found in both complexes, this would be clear evidence that the Chl organization is the same in native and reconstituted complexes and that the only heterogeneity present is the one due to mixed occupancy of some of the Chl binding sites.

MATERIAL AND METHODS

Sample preparation

Native CP29

The native complex was isolated from maize PSII membranes (Berthold et al., 1981) as previously described (Croce et al., 1996). In short, the membranes were solubilized in *n*-docecyl- β -D-maltoside (DM) and then fractionated by nondenaturing flat bed isoelectrofocusing. The green band containing CP29 was harvested and eluted from the gel with 0.06% DM and 50 mM Hepes pH 7.6. The sample was then loaded on a sucrose gradient

(0.1–1M) containing 0.06% DM and 10 mM Hepes pH 7.6. After running 23 h at 39,000 rpm in a SW41 rotor (Beckman) at 4°C it was harvested with a syringe. The sample was analyzed by SDS-page as previously reported (Bassi et al., 1985).

Recombinant CP29

The construct overexpressing maize Lhcb4 was obtained as described earlier (Giuffra et al., 1996) except for a sequence coding for a His₆ tail inserted at the 3' end before the stop codon.

Complex reconstitution was performed as already reported (Giuffra et al., 1996) using Chl a/b ratio of 4.0 and a mixture of all the carotenoids present in the thylakoid membrane. Purification of the reconstituted complex was performed by affinity chromatography on a Ni column followed by ultracentrifugation on glycerol gradient (15–40% glycerol, 0.06% DM, 10 mM Hepes pH 7.6, 12 h at 55,000 rpm in a SW60 rotor; Beckman).

The pigment composition was determined by HPLC analysis (Gilmore and Yamamoto, 1991) and analysis of the absorption spectrum of the acetone extracts was performed with the spectra of the individual pigments (Croce et al., 2002).

Absorption spectra analysis

The absorption spectra of the two samples in the 630- to 720-nm region have been analyzed by deconvolution with the absorption forms of the Chls in protein environment as described (Cinque et al., 2000a). In the description 12 Chl absorption bands are used, eight for Chl a and four for Chl b, in agreement with the results of the mutation analysis (Bassi et al., 1999). The absorption maximum of each band is used as a fixed parameter and it has the value determined by mutation analysis (Bassi et al., 1999). The intensity of the individual bands also reflects the values obtained in the mutation analysis: fixed values representing the absorption of one Chl were used for the “pure” Chl-a sites. For the mixed sites a variation of \pm 10% with respect to the value obtained by mutation analysis was allowed in the analysis of nCP29 to optimize the description. The occupancy (Chl a/Chl b) of the mixed sites obtained with the best fit was: A3 70/30, B3 24/76, B5 58/42, and B6 45/55. For the rCP29, which shows a lower Chl a/b ratio, the intensity of the bands associated with the mixed sites was varied to obtain the best description. In this case, the best description was obtained assigning to the mixed sites the following values (Chl a/Chl b): A3 65/35, B3 16/84, B5 40/60, and B6 30/70. Using this description, it is possible to calculate the direct excitation in the Chl a and Chl b for the two excitation wavelengths used in the experiments. The results obtained convoluting the spectra of the single pigments with the spectrum of the laser pulse (a FWHM 7-nm was used for the analysis) are reported in Table 1.

Femtosecond measurements and analysis

Femtosecond transient absorption was measured as described in (Croce et al., 2001). In short, the pulse width was \sim 60 fs with a spectral width (FWHM)

TABLE 1 Percentage of direct excitation in the different Chl absorption forms, after the excitations at 640 and 653 nm for the two samples

	CP29 native		CP29 recombinant	
	Ex 640	Ex 653	Ex 640	Ex 653
Chl a	30.7%	49.2%	26%	41.9%
Chl b-640	49.5%	13%	49.3%	12.5%
Chl b-652	19.8%	37.8%	24.7%	45.6%

The data were calculated from the description in Fig. 1 convoluting each Chl spectrum with the pulse spectrum (FWHM 7 nm).

of $\sim 7\text{--}8$ nm. Intensities between 0.6 and $1.8 \cdot 10^{13}$ pH/(cm² pulse), depending upon the excitation wavelength, were used. The analysis has been performed by lifetime distribution analysis and is represented as lifetime density maps, as described in that work in detail. To summarize, the lifetime density plots present the amplitudes of the lifetime components in a quasicontinuous lifetime range. White-yellow spots represent positive amplitudes and reflect either decay of an absorption or rise of a bleaching. Blue to black spots represent negative amplitudes and reflect either decay of the bleaching or rise of absorption. In the detection ranges between 640 and 660 nm, strong oscillations occur at early times after excitation ($t < 200$ fs) in the transient traces (compare with Fig. 2). These oscillations, which we believe are not directly due to energy transfer processes of the Chls, have been eliminated from the transient spectra using a special deconvolution procedure. They can, in no way, be described in terms of a sum of exponentials. In summary, we consider the oscillations in the deconvolution procedure as an overdamped oscillation term, which describes the experimental situation sufficiently well, whereas the energy transfer kinetics is still described as a sum of exponentials. As a result of this special deconvolution we obtain the deconvoluted exponential kinetics, free from oscillations, which we present as a modified lifetime density map (or alternatively the deconvoluted kinetics at a particular wavelength).

This deconvolution was specifically designed to correct for the complicated oscillation-like dynamics observed on the early time scale between 640 and 660 nm. At least in part, they most likely arise from some kind of four-wave mixing effects between the pump and probe pulse. We used an extended model function as given in the following equation. This function is actually based on the analysis of oscillatory four-wave mixing effects. However, we stress the point that, quite independently of any actual physical interpretation of these oscillations, an overdamped oscillation term, as used here, accounts very well for the actual observations.

$$\Delta Abs(\lambda, t) = A(\lambda) \times \exp(-i\omega(\lambda)t) \int_t^{+\infty} P(\varphi - s(\lambda)) \times \exp(-(\varphi - t)/\tau_{\text{relx}}) d\varphi + c.c. \\ + \int_{-\infty}^t P(\varphi - s(\lambda)) \int_{\tau} a(\lambda, \tau) \times \exp(-(t - \varphi)/\tau) d\tau d\varphi$$

The second part of the formula corresponds to the conventional, purely exponential model function of the lifetime density approach with amplitudes a and lifetimes τ , whereas the first one and its complex conjugated term accounts in a first approximation for the perturbed free induction decay as well as for off-resonant four-wave mixing effects. These four-wave mixing effects result in some oscillation patterns around zero delay time. When the noncollinear pump and probe pulses overlap, they produce a periodic grating-like excitation that couples them together. If the dephasing time of the polarization induced by the probe pulse is sufficiently long, then a small part of the pump pulse can be scattered into the direction of the probe beam during pump-probe overlap and also at negative delay times, i.e., when the probe pulse arrives prior to the pump pulse. In this first-order approximation these four-wave mixing oscillations are described by a single mean frequency mode varying with the detection wavelength. It is subsequently addressed by an (in time) inversely convoluted exponential term, which represents the dephasing of the polarization generated by the probe pulse in the medium before time zero. A dephasing time τ_{relx} at room temperature of 20 fs was consistently used in the analysis, but is not critical. The phase of the oscillation is determined by the complex value of the amplitude $A(\lambda)$ and its complex conjugated, while the best frequency ω was obtained for each detection wavelength in an iterative process to achieve the lowest χ^2 -value for the fit. The system response function, i.e., the cross-correlation function P , also includes the wavelength-dependent shift s to correct for a chirp of ~ 4 fs/nm in the white-light continuum.

RESULTS

Two complexes were analyzed in this study. The native CP29 has been purified from maize and a recombinant CP29-WT has been reconstituted in vitro using an apoprotein with WT sequence and a mixture of pigments containing all the chromophores present in the thylakoid membrane (Giuffra et al., 1996). The native complex binds 5.9 Chls a and 2.1 Chls b, whereas in the recombinant one there are 5.5 Chls a and 2.5 Chls b. Both complexes bind two carotenoids per polypeptide: $0.8\text{--}0.9$ lutein and $0.5\text{--}0.6$ each of neoxanthin and violaxanthin.

The absorption spectra of native and reconstituted complexes are shown in Fig. 1, *top* and *bottom*. Note that in the recombinant complex more absorption is associated with the Chl b 652 nm. This is an effect produced by the use of a lower Chl a/b ratio in the reconstitution mixture, which allowed obtaining complexes with a somewhat higher Chl b content.

For analyzing the kinetic data it is important to know the initial excitation conditions. To calculate the relative excitation in the different Chls the absorption spectra of the two complexes were described in terms of the absorption of individual chromophores using the spectral forms of Chl a and Chl b in protein environment as described earlier (Cinque et al., 2000a). The absorption maxima of the Q_y transitions were obtained by mutation analysis (Bassi et al.,

1999; see also Fig. 1). This ignores any possible effects of excitonic coupling (see below), but should still be fairly accurate. We have to stress the point that the data shown do not represent the results of a specific fitting of the absorption spectrum in each particular case. Since all the parameters, including the extinction coefficients, Chl contents, and Chl maxima are known, there are no free parameters available for a fit. Taking this into account the agreement of the analysis with the experimental data is more than satisfactory and probably indicates that the effects of excitonic coupling on the absorption spectra are likely to be moderate to small. Using these descriptions, the direct excitation in the individual pigments at the two excitation wavelengths (640 and 653 nm) used in the pump-probe experiments was calculated by convolution of the spectra of individual pigments with the spectrum of the laser excitation pulse. It is clear that, despite four bands being used to describe the Chl b region, according to mutation analysis results only two Chl b pools can be discriminated spectroscopically due to the almost complete superposition of the absorption spectra:

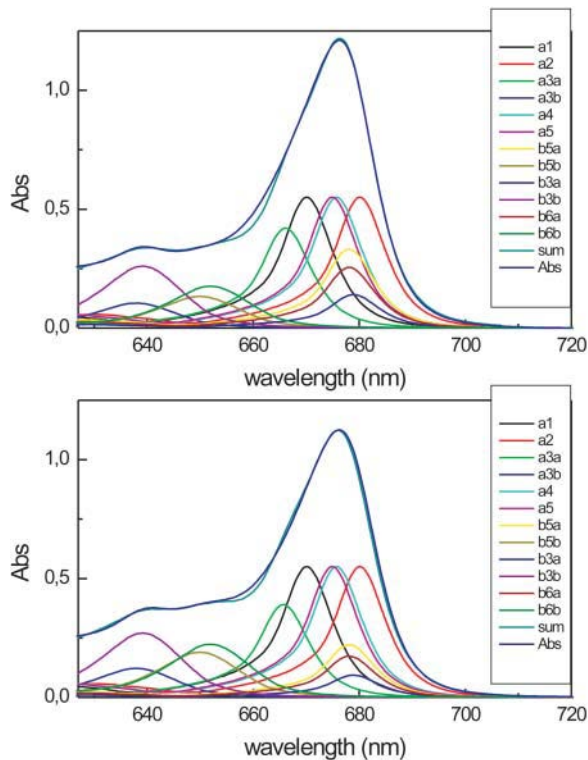


FIGURE 1 Absorption spectra of native (*top*) and reconstituted (*bottom*) CP29. The description of the spectra in terms of absorption of individual Chls is presented. All the spectra of Chl a and Chl b have been multiplied by 2.

a “red Chl b pool” with absorption at 652 nm; and a “blue-Chl b pool” which absorbs ~ 640 nm. The results are presented in Table 1. At both excitation wavelengths, a substantial amount of direct excitation in Chl a is present, which accounts for 20–47% of the total energy absorbed. In the case of the 640-nm excitation the largest part of the energy absorbed by Chl a excites the vibrational side bands of the red Chls a (678–680 nm), which show a maximum ~ 630 nm.

Femtosecond measurements

For both complexes two excitation wavelengths, 640 nm and 652–653 nm, were used to selectively excite the blue and the red Chl-b pools and the kinetics were measured over the 610–730 nm range in a region where the Chls Q_x and Q_y signals are present. In Fig. 2 some selected decay kinetic traces for both excitations are reported.

As noted above (Materials and Methods), particularly in the Chl-b absorption region and up to 670 nm, there are fairly strong oscillations observed which cannot be described in exponential terms, and thus the classical deconvolution description fails. These oscillations not only distort the quality of the fits but also have some influence on any kinetics and spectral components with lifetimes smaller than ~ 200 fs. It is not completely clear why this feature appears in the CP29 measurements whereas it was not present to any

appreciable extent in LHCII measurements. One possible explanation is that, in the case of CP29, the absorption in the Chl b region is not very intense compared to LHCII, due to the presence of only two Chls b, whereas in LHCII there are at least five Chls b which absorb almost all in the 650–652 nm region. Some part of these oscillations is, in our view, also due to vibrational ladder relaxation in the high vibrational states of Chls a. In this article, we do not discuss these oscillation effects in any detail, but rather postpone the discussion to a later work describing individual Chl excited-state relaxation processes. To obtain good insight to the data without loss or distortion of the information, we performed the analysis in three different ways for WT complex: 1), using all the data collected and fitting them as usual as a sum of exponential functions, which clearly is very unsatisfactory and leads to extremely poor fits and distorted ultrafast lifetimes and spectra; 2), cutting off the data on the early time scale (< 150 fs) to eliminate part of the oscillation, which improves the fitting quality but is likely to make it impossible to resolve fast lifetimes up to 200–250 fs; and 3), explicitly including in the analysis a damped oscillation term as described in Materials and Methods. The latter is the preferred analysis mode. While we present and shortly discuss the differences in the lifetime density maps for these methods, we finally use only method 3 to deduce the proper kinetic data.

Fig. 3 shows for the native CP29 complex and for both excitation wavelengths the results of all the analysis methods in terms of lifetime density maps. It is interesting to note that, for the 653-nm excitation, the lifetime density maps obtained are almost identical, independently of the method used in the analysis. This is not true for the 640-nm excitation where up to 200 fs the different analyses give very different results (compare with Fig. 3). Three main kinetic components reflecting energy transfer processes are present for the 640-nm excitation in all the analyses: a transfer from the 640-nm, Chl b to the 675 nm Chl a in 600–800 fs, a transfer from the 652 nm Chl b to 680 nm Chl a in 1–1.2 ps and a third component of 4–6 ps that involves the transfer from 645-, 655-, and 670-nm Chls to red Chl a at 680 nm. In the time scale below 200 fs the analyses show a negative feature in the 635- to 640-nm range with a lifetime, strongly dependent on the analysis method, which ranges between 50 and 130 fs. To interpret this negative feature in Chl-b region as energy transfer it would be necessary to observe an equivalent rise in the Chl a region. Such a rise is hardly detected. In the analysis 1), a positive feature in Chl a region is observed in a time scale faster than the supposed Chl b bleaching decay; in 2), the rise observed at 680 nm is far less intense than the decay at 640 nm; and in 3), it is absent. Note that, for all the analysis, the region above 200 fs is very similar.

The 653-nm excitation shows at least three different lifetimes: 100- to 150-fs transfer from 652 nm Chl b to 680 nm Chl a; a second transfer from 652 nm to 678 nm in 800–1 ps; and a third one of 5–6 ps. An equilibration between Chl a

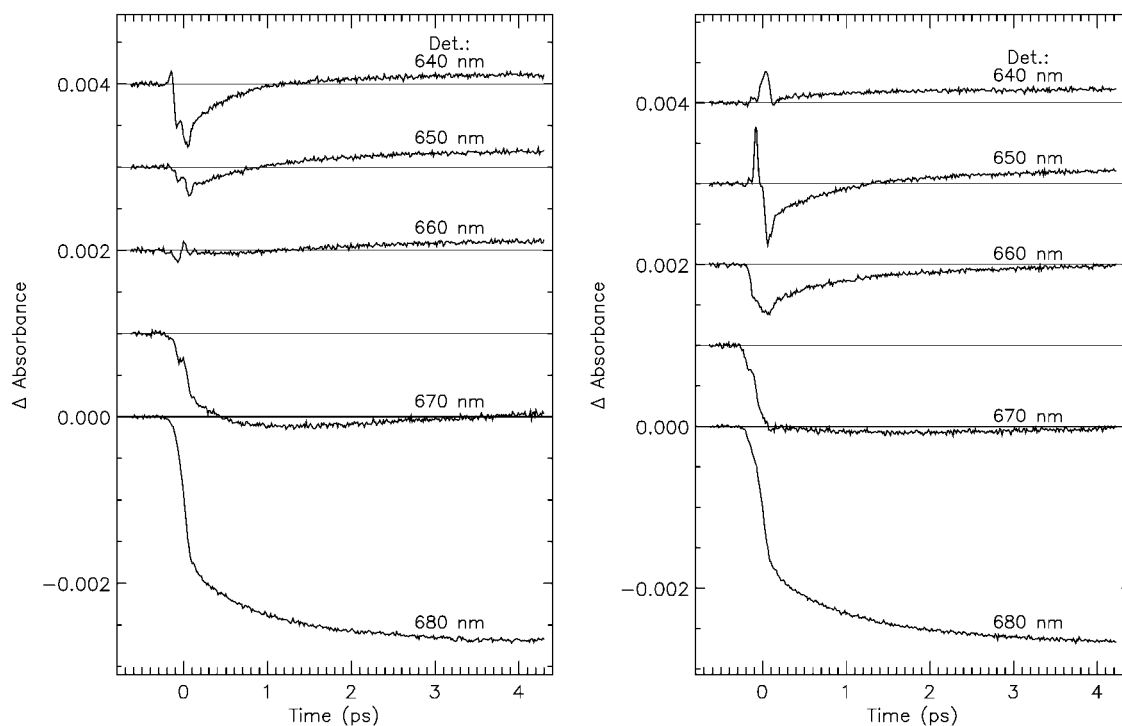


FIGURE 2 Experimental transient absorption kinetics at selected detection wavelengths for nCP29 complex. (*left*) Excitation at 640 nm; (*right*) excitation at 653 nm.

molecules is present with 6-ps lifetime as in the case of 640-nm excitation. These components can be observed in all the analysis performed. The positive and negative components detected in the 640-nm region of 100 and 250 fs, respectively, are probably an artifact of the conventional analysis due to the presence of the oscillation which is particularly pronounced \sim 640 nm as shown in Fig. 2.

In Fig. 4 the lifetimes' density maps for recombinant CP29 are reported. In this case, only the result of the modified analysis procedure (method 3) is presented. All the kinetic components are, in fact, very similar to what is observed in the native complex, except for the presence of more pronounced transfer components from the 652 nm Chl b upon excitation at 640 nm. This is related to the higher absorption at 652 nm in the rCP29 (Fig. 1), which reflects the presence of additional 0.5 Chl-b molecules in this sample compared to nCP29, allowing exciting directly more Chl b 652 nm, as compared to the native complex upon 640-nm excitation (see Table 1). The main transfer from the 640 nm Chl b is observed with 600- to 800-fs lifetime, whereas three transfers at 100–150 fs, 1–1.2 ps, and 5–6 ps are still detected for the 652-nm excitation and again a component of 6–8 ps corresponds to the equilibration between Chl a-670 nm and Chl a-680 nm.

DISCUSSION

Analysis of CP29, reconstituted with different Chl a/b ratios (Giuffra et al., 1997), and the mutation analysis performed

on CP29, selectively substituting the Chl binding residues with amino acids which are not able to coordinate Chls, have suggested that Chl b is accommodated in four different sites (Bassi et al., 1999), although on average only two Chls b are present in the complex. This implicates that in CP29 four out of the eight Chl binding sites do not have a strong preference for either Chl a or Chl b. These sites have been named mixed sites. Whereas the evidence for the presence of these mixed sites is quite strong for the recombinant complex rCP29, some doubt still remains about their presence in the native complex. To sort out this point, we performed energy transfer measurements on both the reconstituted and the native CP29 complexes and compared the results. If in the native CP29 the Chls b are coordinated in only two sites, only two kinetic components for the Chl b to Chl a transfer are expected: one from the Chl b at 640 nm and a second one for the Chl b at 652 nm. If sites with mixed occupancy are present, more than two components for Chl b to Chl a transfer are expected.

The 652-nm excitation

The 652- to 653-nm excitation of both native and reconstituted CP29 gives identical results. Three kinetic components for the Chl b-652 nm to Chl a transfer can be identified in the measurements: a fast one with 100–200 fs, a second one with an \sim 1.2-ps lifetime and a third one with a 5- to 6-ps lifetime. These results clearly indicate that the Chl organization in the two complexes is the same. Not only

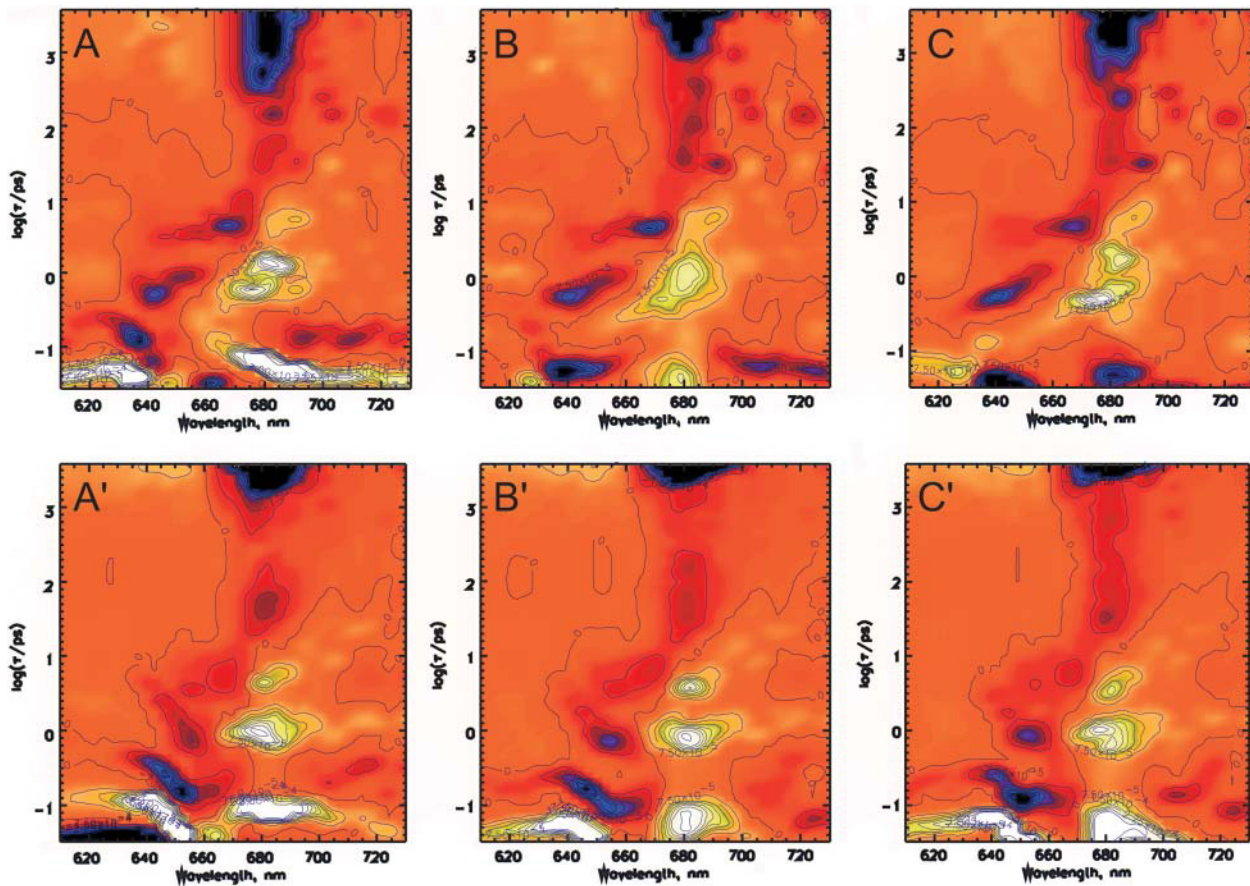


FIGURE 3 Lifetime density maps of native CP29 complex excited at 640 nm (*top*) and 653 nm (*bottom*). Three analyses are shown: (A-A') using all the collected data and fitting them in exponential terms; (B-B') using the data collected after 80 fs only; and (C-C') analyzing all the data, by applying a deconvolution procedure taking into account a damped oscillation term (see text for details).

do the Chls absorb at the same wavelengths, as already indicated by steady-state spectroscopy analysis (Giuffra et al., 1996, 1997), but also the orientation of the dipole moments is conserved in the reconstituted complex as compared to the native one, thus yielding identical transfer kinetics. Even more important, three components have been detected for the transfer from Chl b-652 nm to Chls a, strongly indicating that the absorption ~ 652 nm originates from Chls b accommodated in more than two sites. This observation points to a unique conclusion: the mixed sites exist also in the native complex and the relative occupancies are quite similar, except for the somewhat higher total Chl-b content of the rCP29 complex.

Previous measurements on native CP29 showed for the 652 nm Chl b form a single decay only in ~ 2.2 ps. The discrepancy with our results is not surprising, since the instrument resolution in those measurements was near 200 fs (Gradinaru et al., 1998). More recently, the same group performed a femtosecond transient absorption study on carotenoid to Chl energy transfer on CP29. In this work, they were able to observe two distinct energy transfers from Chl b-652 nm in 2.2 ps and 9.8 ps (Gradinaru et al., 2000). Again, the fast transfer time was absent as compared to our data.

This can easily be explained, taking into account that the measurements were carried out with carotenoid excitation, and thus the kinetics were more complex due to the simultaneous presence of car to Chl and Chl b to Chl a transfers. Doing similar measurements, we were able to see a fast transfer from car to Chl-b 652 nm in ~ 100 fs (Croce et al., 2003). Considering that the lifetimes for the transfer from car to Chl b and from Chl b to Chl a are very similar, it is almost impossible to resolve the Chl b to Chl a transfer in 100–200 fs following carotenoid excitation. The lack of Gradinaru et al. (2000) to resolve the fast transfer step even in high-resolution experiments upon carotenoid excitation is thus not in disagreement with our data, which clearly suggest such a fast Chl b to Chl a transfer step. In Table 2 a comparison between the energy transfer kinetic components observed by different groups for CP29 complex is presented.

The 640-nm excitation

Due to the oscillatory contribution for 640-nm excitation, which seems to be particularly strong in the wavelength region between 640 and 660 nm, we cannot completely exclude an energy transfer component from the 640 nm Chl b

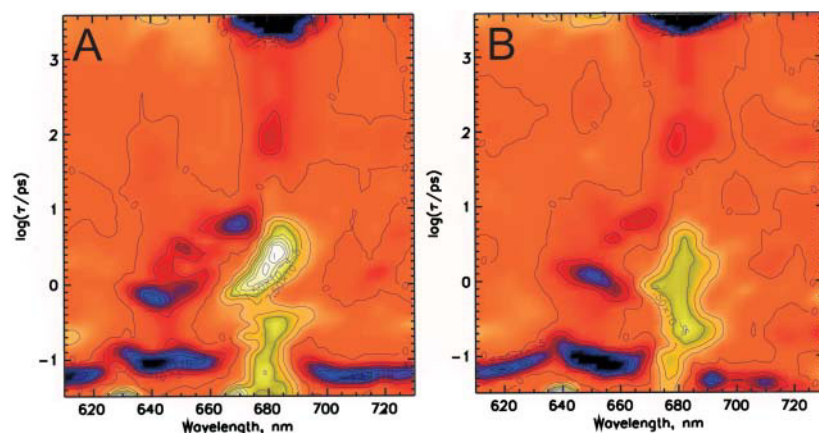


FIGURE 4 Lifetime density maps of the reconstituted CP29 complex: (A) excitation at 640 nm; (B) excitation at 652 nm. The deconvolution procedure used is method C of Fig. 3.

of ~ 100 fs. However, taking into account the complete picture our observations suggest that the negative feature observed at 635 nm in the 50–150 fs decay range is not associated to a bleaching decay of the 640-nm Chl-b form, but it is likely to be a Chl a vibrational relaxation. This is supported by the strong dependence of this feature upon the analysis methods used, and it can be eliminated when the oscillation is taken into account explicitly. Previous experiments on nCP29 have shown a very fast decay of the 640-nm form in 220 fs, which accounted for 60% of the energy, a second decay (20% of the energy) in 2.2 ps and a third one (20%) in 9.8 ps (Gradinaru et al., 2000). These results have been obtained by SADS global analysis of the carotenoid excitation (489 nm) and the low number of components used to fit the entire region between 632 and 658 nm can explain the difference in lifetimes to our results. Interestingly, the same authors, exciting the sample at 506 nm, found only one transfer time from 640 nm Chl b, which happened in less than 150 fs, whereas the slow components which they were able to resolve after the excitation at 489 nm were practically absent. Moreover, comparing the excitation at 489 nm, where a large part of the energy reached Chl b directly, with the 506-nm excitation, where less Chl b is directly excited, the value for the total Chl b direct excitation was identical to the ratio of the immediate bleaching between the Chl b 640

nm and Chl b 652 nm forms. This is quite surprising because two separate Soret band positions are believed to be associated with the 640-nm and 652-nm Chl b and the excitation is thus expected to be more selective (Croce et al., 2003). The two observations, i.e., the fact that the bleaching at 640 nm was quite strong after excitation at 506 nm (where low Chl b direct excitation is expected) and the fact that this bleaching decayed mainly with a lifetime shorter than 150 fs, whereas the slow component was not present, can also suggest that the feature at 640 nm in the work of Gradinaru et al. (2000) is at least partially associated with the vibrational relaxation of Chl a. In effect, the 506-nm excitation is expected to directly excite Chl a, more so than at 489 nm.

In our measurements, the main transfer component out of Chl b 640 nm shows a lifetime of 600–800 fs in both samples. A very small amplitude component of ~ 4 ps is also present, whereas this component is more clearly visible upon Soret excitation (Croce et al., 2003). This component probably corresponds to the 9.8-ps component reported by Gradinaru et al. (2000), also upon Soret excitation. There are also evidences for weak lifetimes components above 10 ps (see Figs. 3 and 4). We note, however, that these long lifetimes might be related not so much to energy transfer but to conformational reorganization. Measurements on some of the mutants of CP29 that lack single Chls (data not shown) also show a component of 4 ps, although maintaining the 600- to 800-fs transfer as the main component in the 640 nm Chl b decay.

TABLE 2 Energy transfer kinetic components for CP29 complex according to different studies

	This article	Gradinaru et al. (1998, 2000)	Pieper et al. (2000)
Chl b-640	600–800 fs (4 ps)	220 fs (350 fs) 2.2 ps 9.8 ps	900 fs
Chl b-652	150 fs 1.2 ps 5–6 ps	2.2 ps 9.8 ps	4.2 ps
Chl a-670	1 ps 6–8 ps	280 fs 10–13 ps	4.3 ps

Lifetime assignments to individual Chl binding sites

The energy transfer process in the CP29 complexes to a first approximation can be analyzed based on the Förster mechanism, although some exciton coupling effects will be present, as pointed out previously (Iseri et al., 2000; Voigt et al., 2002). For Förster-type transfer the main parameters that influence the transfer rate are: the distance between the chromophores, the overlap between the fluorescence of the

donor, and the relative absorption of the acceptor and the orientation of the dipole moment transitions (Förster, 1965). It is the attraction of the simple Förster description that, in the case of CP29, all these parameters are known; the distance between Chl was obtained from the structure of LHCII (Kühlbrandt et al., 1994), which is a highly homologous complex. The energy of the S_1 electronic levels for all Chls has been determined by mutation analysis and differential spectroscopy (Bassi et al., 1999), and the orientation of the dipole moments has been determined by LD analysis on the mutant complexes which lack, selectively, single Chls (Simonetto et al., 1999). Using those data, it has been possible to calculate the energy transfer processes in the complex in the Förster approximation (Cinque et al., 2000b). The calculations indicate that for the 652-nm Chl b form two main transfer components are expected: a fast one in 160–180 fs and a slow one in 1.4–1.7 ps. The fast transfer should be associated with the Chl b in site B5 whereas the slow one is attributed to the transfer from Chl b in site B6. The range of expected lifetimes obtained from the calculations is due to the fact that, considering four mixed sites, 16 different populations should be present in the sample, each one having a particular set of lifetimes for the transfer of each particular Chl due to the different occupancy in the neighboring sites. Our experimental lifetimes are practically identical with the calculated ones, which strongly supports the overall model.

The calculations suggest also two main decays for the 640-nm, Chl b forms. The first one of 1.7 ps should be associated with Chl b in site B3 and a slower one of 6 ps should be associated with Chl b in site A3 (Cinque et al., 2000a,b). In this case, the mutation analysis showed that the affinity for Chl b in site A3 is $\sim 30\%$, whereas it is 70% in site B3. It is thus expected that the faster decay dominates the kinetics. The experimental data show a decay in the lifetime range of 600–800 fs. This is by a factor of 2 faster than the calculations suggested. The reason for this discrepancy might be that the relative orientation of transition moments in the A3/B3 sites might be different than concluded by Cinque et al. (2000b). We note, however, that in Simonetto et al. (1999) it was not possible to determine directly by LD spectroscopy the orientation of the A3 site, due to the low quality of the spectrum, and thus A3 orientation was obtained from the fit of the LD spectrum. It is also possible that the discrepancy in lifetimes is due to the importance of exciton interaction as suggested by Iseri and co-workers (Iseri et al., 2000).

The mixed sites in CP29

Aiming to further test the mixed site hypothesis the recombinant CP29 used in our measurements was reconstituted with a low Chl a/b ratio to obtain a complex that binds more Chl b than the native one. It is well known, when reconstituting *in vitro*, that it is possible to modify the Chl a/b ratio in the folded complex using different pigment mix-

tures during the reconstitution procedure (Giuffra et al., 1996, 1997; Pagano et al., 1998; Croce et al., 2002; Kleima et al., 1999). The native CP29 has a Chl a/b ratio of 2.8, meaning 5.9 Chls a and 2.1 Chls b, whereas the reconstituted complex shows a final Chl a/b ratio of 2.2, i.e., 5.5 Chls a and 2.5 Chls b. In the reconstituted complex there is thus a substitution of 0.4 Chl a by 0.4 Chl b with respect to the native one. Our aim was to check if the substitution in the recombinant complex is uniform in all sites or if the first sites to be substituted are the mixed sites. In the first case we expect to see additional Chl b to Chl a components in the reconstituted sample as compared to the native one, while the same components, but with different intensity ratio, are expected if the substitutions are in the mixed sites only. No additional components are observed in the recombinant complex; moreover, the 640-nm excitation clearly indicates that more Chl b 652 nm is excited at this wavelength in the reconstituted complex compared to the native. It is thus clear that the Chl a to Chl b substitution occurs in one site preferentially, which already accommodates Chl b in the native complex, with its absorption maximum tuned to 652 nm (sites B5 and B6). This result provides additional evidence for the existence of specific mixed sites in the native CP29 complex.

CONCLUSIONS

For both samples the same kinetic components have been found, indicating that the organization of the Chls in the native and recombinant CP29 is very similar in terms of distance between chromophores, absorption energy of pigments in specific sites, and orientation of the dipole moments. At least four components are associated with the Chl b to Chl a energy transfer in both the native and the reconstituted complex, indicating the presence of four sites with mixed Chl a/b occupancy. The equilibration among the Chls a occurs with several time constants with main components ranging from ~ 1 ps and 6–8 ps (670-nm excitation; data not shown). Weak lifetime components, present in the data above 10 ps and up to several hundred ps, cannot be identified clearly as energy transfer components. It is more likely that these long-lived components reflect conformational reorganization processes in the protein environment upon excitation. Overall, the agreement of the Förster calculations (Cinque et al., 2000b) with the experimental data is surprisingly good. This suggests that the Förster model is quite a reasonable first order approximation. It will have to be amended eventually with an improved theory considering exciton coupling effects for at least one or two Chl pairs, as is suggested by the work of Iseri (Iseri et al., 2000).

R.C. was supported by a TMR Marie Curie Fellowship Grant ERBFM-BICT983216 from the European Union. We also thank the Deutsche Forschungsgemeinschaft (SFB 189, Heinrich-Heine-Universität Düsseldorf, and Max-Planck-Institut für Strahlenchemie) for financial support.

REFERENCES

- Bassi, R., and S. Caffarri. 2000. LHC proteins and the regulation of photosynthetic light harvesting function by xanthophylls. *Photosynth. Res.* 64:243–256.
- Bassi, R., R. Croce, D. Cugini, and D. Sandona. 1999. Mutational analysis of a higher plant antenna protein provides identification of chromophores bound into multiple sites. *Proc. Natl. Acad. Sci. USA.* 96:10056–10061.
- Bassi, R., O. Machold, and D. Simpson. 1985. Chlorophyll-proteins of two photosystem I preparations from maize. *Carlsberg Res. Commun.* 50:145–162.
- Berthold, D. A., G. T. Babcock, and C. F. Yocum. 1981. A highly resolved, oxygen-evolving photosystem II preparation from spinach thylakoid membranes. EPR and electron-transport properties. *FEBS Lett.* 134: 231–234.
- Boekema, E. J., H. van Roon, F. Calkoen, R. Bassi, and J. P. Dekker. 1999. Multiple types of association of photosystem II and its light-harvesting antenna in partially solubilized photosystem II membranes. *Biochemistry.* 38:2233–2239.
- Cinque, G., R. Croce, and R. Bassi. 2000a. Absorption spectra of chlorophyll a and b in Lhcb protein environment. *Photosynth. Res.* 64:233–242.
- Cinque, G., R. Croce, A. R. Holzwarth, and R. Bassi. 2000b. Energy transfer among CP29 chlorophylls: calculated Förster rates and experimental transient absorption at room temperature. *Biophys. J.* 79:1706–1717.
- Croce, R., J. Breton, and R. Bassi. 1996. Conformational changes induced by phosphorylation in the CP29 subunit of photosystem II. *Biochemistry.* 35:11142–11148.
- Croce, R., G. Canino, F. Ros, and R. Bassi. 2002. Chromophores organization in the higher plant photosystem II antenna protein CP26. *Biochemistry.* 41:7334–7343.
- Croce, R., M. G. Müller, R. Bassi, and A. R. Holzwarth. 2001. Carotenoid-to-chlorophyll energy transfer in recombinant major light-harvesting complex (LHCII) of higher plants. I. Femtosecond transient absorption measurements. *Biophys. J.* 80:901–915.
- Croce, R., M. G. Müller, S. Caffarri, R. Bassi, and A. R. Holzwarth. 2003. Energy transfer pathways in the minor antenna complex CP29 of Photosystem II: a femtosecond study of carotenoid to chlorophyll transfer on mutant and WT complexes. *Biophys. J.* 84:2517–2532.
- Förster, T. 1965. Delocalized excitation and excitation transfer. In *Modern Quantum Chemistry, Part III, Action of Light and Organic Crystals*. O. Sinanoglu, editor. Academic Press, New York. pp. 93–137.
- Gilmore, A. M., and H. Y. Yamamoto. 1991. Zeaxanthin formation and energy-dependent fluorescence quenching in pea chloroplasts under artificially mediated linear and cyclic electron transport. *Plant Physiol.* 96:635–643.
- Giuffra, E., D. Cugini, R. Croce, and R. Bassi. 1996. Reconstitution and pigment-binding properties of recombinant CP29. *Eur. J. Biochem.* 238:112–120.
- Giuffra, E., G. Zucchelli, D. Sandona, R. Croce, D. Cugini, F. M. Garlaschi, R. Bassi, and R. C. Jennings. 1997. Analysis of some optical properties of a native and reconstituted photosystem II antenna complex, CP29: pigment binding sites can be occupied by chlorophyll a or chlorophyll b and determine spectral forms. *Biochemistry.* 36:12984–12993.
- Gradinaru, C. C., A. A. Pascal, F. van Mourik, B. Robert, P. Horton, R. van Grondelle, and H. Van Amerongen. 1998. Ultrafast evolution of the excited states in the chlorophyll a/b complex CP29 from green plants studied by energy-selective pump-probe spectroscopy. *Biochemistry.* 37:1143–1149.
- Gradinaru, C. C., I. H. M. van Stokkum, A. A. Pascal, R. van Grondelle, and H. Van Amerongen. 2000. Identifying the pathways of energy transfer between carotenoids and chlorophylls in LHCII and CP29. A multicolor, femtosecond pump-probe study. *J. Phys. Chem. B.* 104: 9330–9342.
- Hankamer, B., J. Barber, and E. J. Boekema. 1997. Structure and membrane organization of photosystem II in green plants. *Annu. Rev. Plant Physiol. Plant Mol. Biol.* 48:641–671.
- Iseri, E., D. Albayrak, and D. Gülen. 2000. Electronic excited states of the CP29 antenna complex of green plants: a model based on exciton calculations. *J. Biol. Phys.* 26:321–339.
- Jansson, S. 1999. A guide to the LHC genes and their relatives in Arabidopsis. *Trends Plant Sci.* 4:236–240.
- Kleima, F. J., S. Hobe, F. Calkoen, M. L. Urbanus, E. J. G. Peterman, R. van Grondelle, H. Paulsen, and H. Van Amerongen. 1999. Decreasing the chlorophyll a/b ratio in reconstituted LHCII: Structural and functional consequences. *Biochemistry.* 38:6587–6596.
- Kühlbrandt, W., D. N. Wang, and Y. Fujiyoshi. 1994. Atomic model of plant light-harvesting complex by electron crystallography. *Nature.* 367:614–621.
- Pagano, A., G. Cinque, and R. Bassi. 1998. In vitro reconstitution of the recombinant photosystem II light-harvesting complex CP24 and its spectroscopic characterization. *J. Biol. Chem.* 273:17154–17165.
- Pieper, J., K. D. Irrgang, M. Ratsep, J. Voigt, G. Renger, and G. J. Small. 2000. Assignment of the lowest Q(Y)-state and spectral dynamics of the CP29 chlorophyll A/B antenna complex of green plants: A hole-burning study. *Photochem. Photobiol.* 71:574–581.
- Sandona, D., R. Croce, A. Pagano, M. Crimi, and R. Bassi. 1998. Higher plants light harvesting proteins. Structure and function as revealed by mutation analysis of either protein or chromophore moieties. *Biochim. Biophys. Acta.* 1365:207–214.
- Simonetto, R., M. Crimi, D. Sandona, R. Croce, G. Cinque, J. Breton, and R. Bassi. 1999. Orientation of chlorophyll transition moments in the higher-plant light-harvesting complex CP29. *Biochemistry.* 38:12974–12983.
- Testi, M. G., R. Croce, P. Poverino-De Laureto, and R. Bassi. 1996. A CK2 site is reversibly phosphorylated in the photosystem II subunit CP29. *FEBS Lett.* 399:245–250.
- Van Amerongen, H., and R. van Grondelle. 2001. Understanding the energy transfer function of LHCII, the major light-harvesting complex of green plants. *J. Phys. Chem. B.* 105:604–617.
- Voigt, B., K. D. Irrgang, J. Ehlert, W. Beenken, G. Renger, D. Leupold, and H. Lokstein. 2002. Spectral substructure and excitonic interactions in the minor photosystem II antenna complex CP29 as revealed by nonlinear polarization spectroscopy in the frequency domain. *Biochemistry.* 41: 3049–3056.